JOURNAL OF MATERIALS SCIENCE 9 (1974) 184–192

An electron-microscopic study of precipitation (exsolution) in an amphibole (the hornblende-grunerite system)

M. F. GITTOS, G. W. LORIMER
Department of Metallurgy
P. E. CHAMPNESS
Department of Geology, Faculty of Science, University of Manchester, UK

Transmission, analytical and high-voltage electron microscopy have been used to study the distribution of phases in the naturally occurring silicate minerals hornblende and grunerite. These two minerals belong to the amphibole group and previous analytical work has suggested the existence of a miscibility gap between them involving the segregation of calcium. The minerals in the specimens studied are coarse-grained, having crystallized slowly during metamorphism.

Large lamellar precipitates are present in both phases. These precipitates form on (100) and ($\bar{1}$01) planes of the matrix and have remained coherent. Steps are present on the broad faces of these lamellae, suggesting that they have thickened by the propagation of ledges as observed in metal alloy systems. These features are common to both phases, but the grunerite matrix contains an additional set of fine, coherent precipitates which have formed at a later stage and show distinct precipitate-free zones around the earlier precipitates. Analytical microscopy has been used to confirm qualitatively that the precipitation involves segregation of calcium.

1. Introduction

The amphibole group of minerals are double chain silicate structures with the general formula $AX_2Y_5Z_8O_{22}(OH, F)_2$ where A = K, Na or a vacancy, X = Na, Ca, Mg or Fe^{2+}, Y = Mg, Fe^{2+}, Fe^{3+} or Al, Z = Si or Al. The anthophyllite-cummingtonite sub-group have the X and Y positions occupied by Mg or Fe^{2+}; the anthophyllites are orthorhombic and contain less than 30% Fe^{2+} in the X and Y positions, while above 30% Fe^{2+} the structure is monoclinic, $C2/m$, and known as cummingtonite. Iron-rich members are known as grunerite*. The hornblende sub-group have the X position occupied by Ca and Mg or Fe^{2+} in the Y position. These calcium amphiboles are also monoclinic, $C2/m$, tremolite being chemically the simplest, $Ca_2Mg_5[Si_8O_{22}](OH, F)_2$. Hornblende has some aluminium substituted for magnesium with the consequent replacement of Si by Al to retain the charge balance. The approximate composition fields of these amphiboles are shown in Fig. 1. In many rocks there is a sharp discontinuity in composition between co-existing hornblende or actinolite and grunerite or cummingtonite, Fig. 1, which suggests that there is a miscibility gap between the two phases. The existence of such a gap is supported by the widespread observations of exsolution lamellae in the optical microscope. The lamellae are generally found to lie on ($\bar{1}$01) and (100) of the matrix.

The object of the present investigation was to use the high resolution tool of transmission electron microscopy to study the distribution of phases in a hornblende containing exsolved grunerite and a grunerite containing exsolved hornblende.

*Cummingtonite and grunerite have a continuous range of composition, Fig. 1. The nomenclature of the series is not precisely defined [1] and so in this paper Ca-poor phases are called grunerite since the iron contents are high.

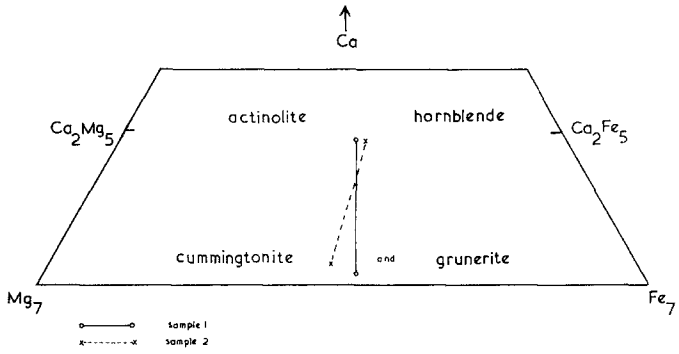

Figure 1 Composition diagram of the anthophyllite-cummingtonite sub-group of amphiboles showing approximate positions of hornblende and grunerite. The composition of specimens 1 and 2 are plotted on the diagram.

2. Experimental

Two rock samples have been examined during the present investigation. Sample 1 was obtained from a grunerite-hornblene-plagioclase schist, Mangha Chrome mining district, Sierra Leone. This material has been analysed by Klein [2] as assemblage 5-21 and is from the collection of S.O. Agrell (No. 80409). Sample 2 is from a metamorphic assemblage in which hornblende and cummingtonite co-exist. It is from the Orange Area Massachusetts and has also been analysed by Klein [2] as assemblage 5-18. The sample was originally reported by Robinson [3] and is No. 7A8B of his collection. The composition of these specimens is plotted on Fig. 1. The analyses of sample 1 and 2 are given in Table I.

TABLE I Analyses of amphibole specimens [2].

	Sample 1		Sample 2	
	H	G	H	G
SiO_2	45.0	51.1	44.1	52.3
Al_2O_3	11.0	1.4	12.0	2.1
FeO	19.8	28.4	20.2	25.1
MnO	0.3	0.7	0.3	0.6
MgO	10.1	15.0	9.3	14.9
CaO	11.0	1.0	9.0	1.4
Na_2O	1.0	0	1.9	0.2
Total	98.2	97.6	96.8	96.6

Doubly polished thin sections were prepared and amphibole grains exhibiting exsolution when viewed in the optical microscope (Fig. 2) were selected for electron microscopic investigation. Thin foils for electron microscopy were prepared by ion-thinning using the techniques described by Barber [4] and Champness and Lorimer [5]. The specimens were then examined in the electron microscope at an accelerating voltage of 100 kV. Selected specimens were also examined in an AEI EM7 high-voltage electron microscope operating at 1000 kV. The combination of ion-thinning and high-voltage electron microscopy proved to be valuable when determining the distribution of phases over areas of several square microns. Qualitative analysis of some of the exsolution lamellae was carried out using the analytical electron microscope EMMA-4.

3. Optical and electron petrography

3.1. Hornblende containing grunerite lamellae

Fig. 2c is an optical micrograph of an ion-thinned grain of hornblende containing grunerite lamellae. Two sets of exsolution lamellae are visible and these correspond to the $(\bar{1}01)$ and (100) lamellae which have been observed by other workers*[6]. Fig. 3a is an electron micrograph of specimen 2 in which $(\bar{1}01)$ and (100) grunerite lamellae are clearly resolved. Fig. 3b is a diffraction pattern from (100) and $(\bar{1}01)$ lamellae and the surrounding matrix in which the electron beam is approximately parallel to $(\bar{1}01)$. From this diffraction pattern it can be seen that for the $(\bar{1}01)$ lamellae the $(\bar{1}01)$

*Reference to the habit planes of the lamellae being "$(\bar{1}01)$" and "(100)" does not imply that the interfaces are exactly parallel to these planes. From careful optical measurements Robinson *et al* [7] found that the habit planes in specimen 2 were up to 3.5° from $(\bar{1}01)$. Owing to the inaccuracy involved in determining crystallographic directions on electron micrographs, we have not made detailed measurements of habit plane orientations.

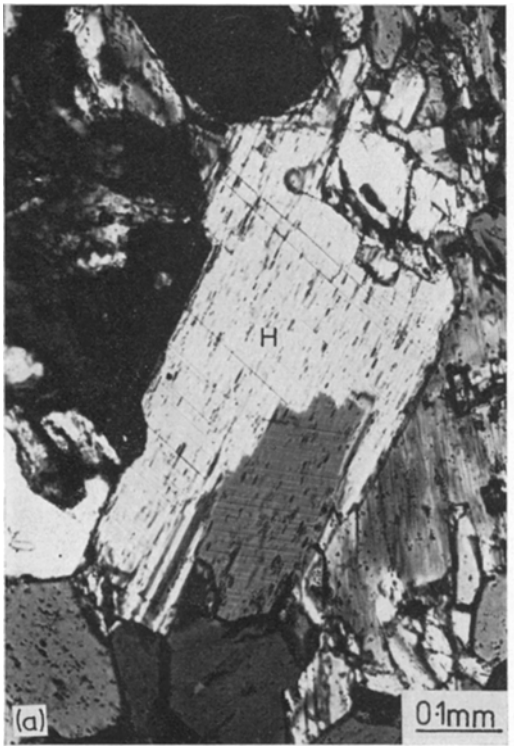

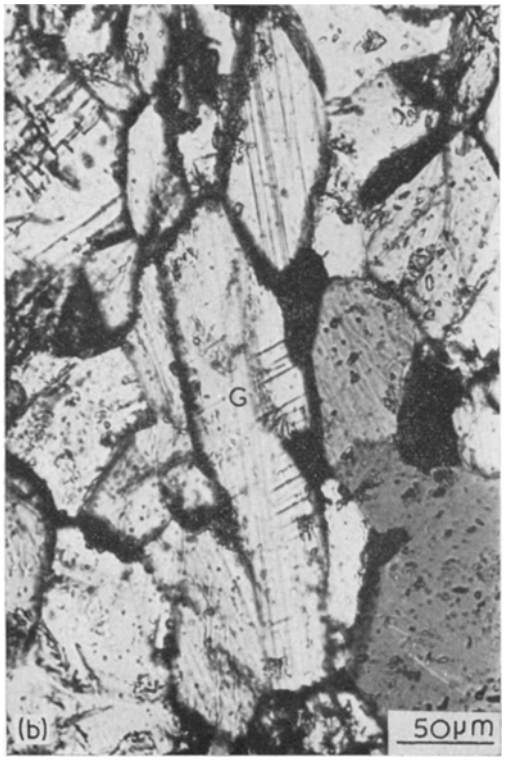

Figure 2 Optical micrographs of thin sections of sample 1 showing, (a) hornblende containing grunerite and (b) grunerite containing hornblende lamellae. (c) Optical micrograph of sample shown in (a) after ion thinning. The ($\bar{1}01$) and (100) exsolution lamellae are clearly visible. The bumpy surface produced by ion thinning is evident.

lattice planes are parallel in the two phases, confirming previous X-ray diffraction studies [6]. Similarly, for the (100) lamellae the (100) lattice planes of the two phases were found to be parallel.

The lattice parameters of the hornblende and grunerite are similar: for hornblende $a = 9.8$ Å, $b = 18.0$ Å, $c = 5.3$ Å, $\beta = 105°$ and for grunerite $a = 9.5$ Å, $b = 18.1$ Å, $c = 5.3$ Å, $\beta = 102°$. Robinson *et al* [7] have shown, by measuring cell dimensions of the intergrown phases, that for the ($\bar{1}01$) lamellae, the ($\bar{1}01$) lattice planes have the minimum misfit, and similarly that for (100) exsolution lamellae (100) is the plane of best fit. That the misfit in the two cases is extremely small is confirmed by our observations that the lamellae are completely coherent (i.e. the lattice planes of the precipitate and matrix are continuous across the interface) even for lamellae up to 0.5 μm thick as can be

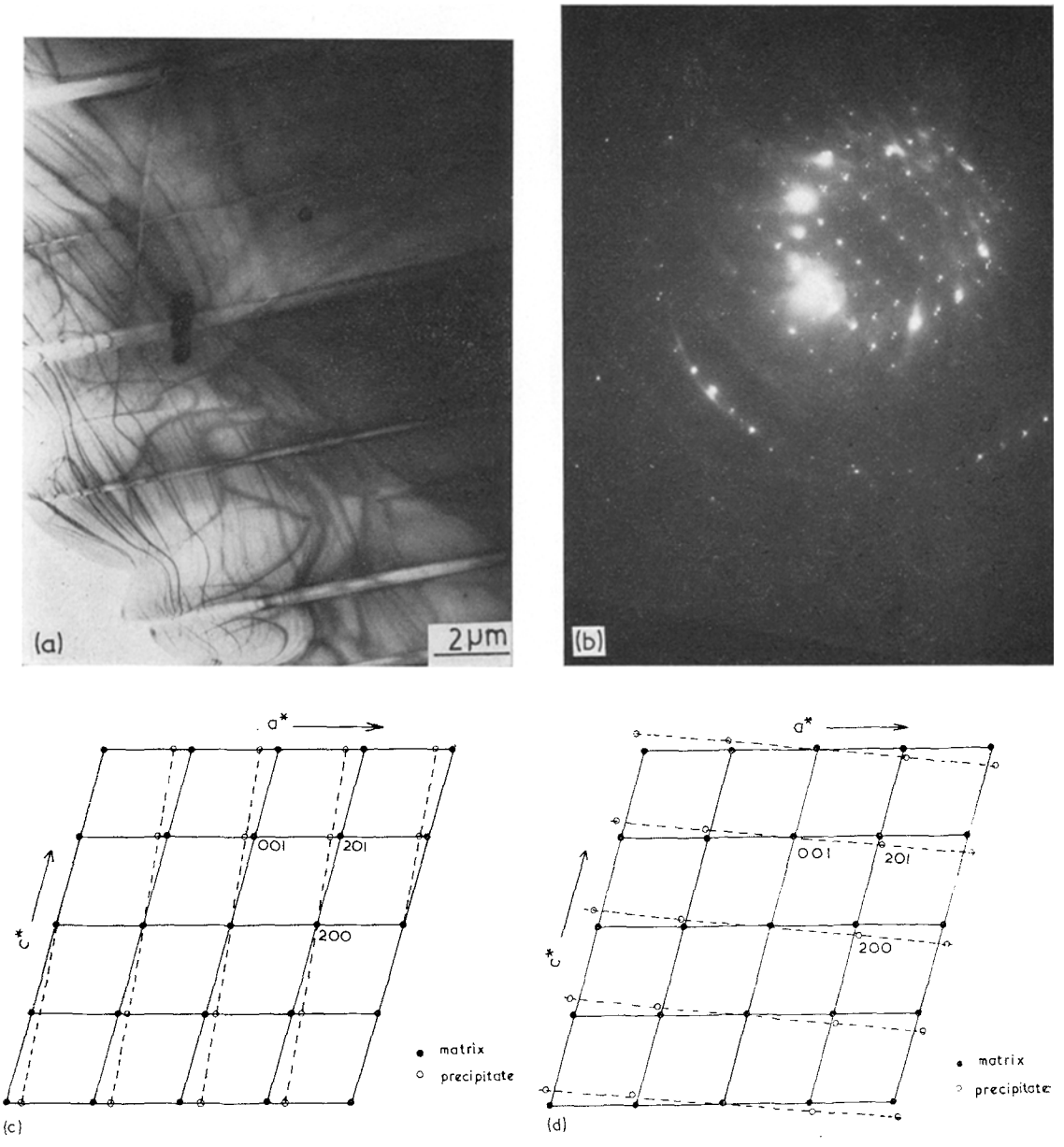

Figure 3 (a) Electron micrograph (100 kV) of ion-thinned grain from specimen 2 showing ($\bar{1}01$) and (100) grunerite lamellae in hornblende. The contamination spots have been produced during the analysis with EMMA-4. (b) Diffraction pattern from grunerite lamellae and hornblende matrix. (c) and (d) Indexed diffraction pattern showing orientation relationships for (c) ($\bar{1}01$) lamellae and (d) (100) lamellae.

seen by the examination of the interface (Fig. 4a and b).

While the (100) interface between the matrix and the lamellae is coherent, irregularly-spaced steps or ledges are often observed at the interface. These steps are clearly resolved when the electron beam is parallel to (100) (Fig. 4a) and they appear as lines when the broad faces of the lamellae make a large angle with the electron beam (Fig. 4b). Similar ledges have been observed at the interfaces of (100) lamellae of exsolved augite in orthopyroxene [8] and in

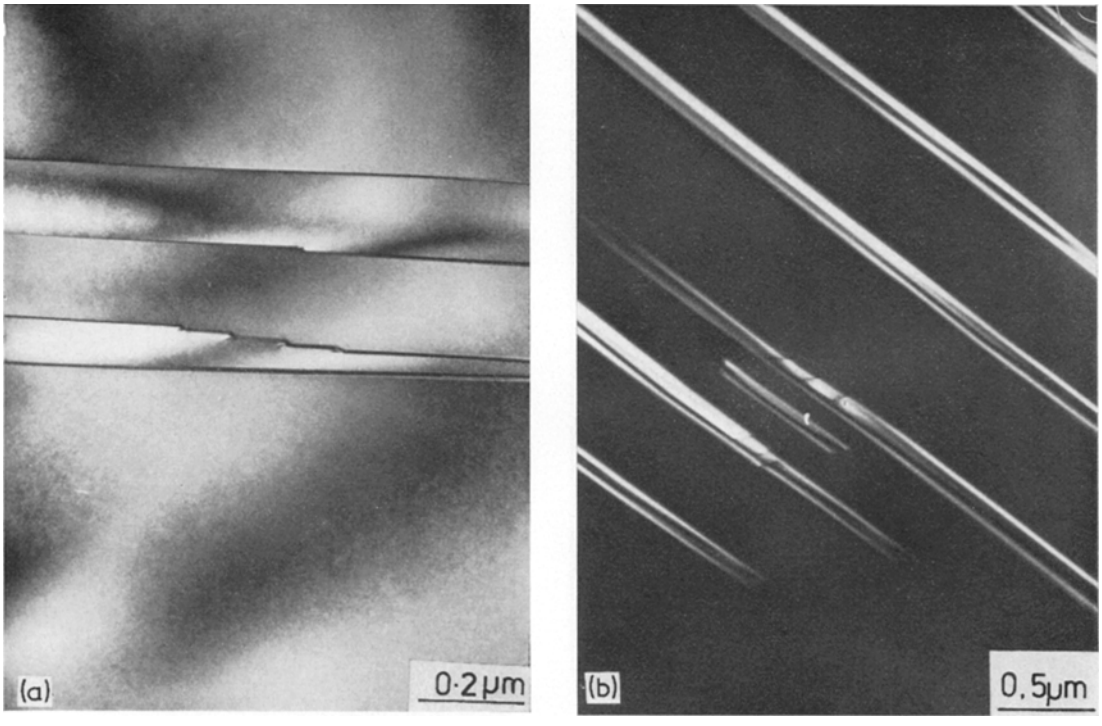

Figure 4 Grunerite lamellae in hornblende showing growth ledges (a) and coherent precipitate/matrix interface (b) with growth ledges.

iron-rich clinopyroxenes containing pigeonite exsolved on (001) [9].† These authors interpreted the ledges as growth features and we propose that the ledges shown in Fig. 4a and b have the same origin.

3.2. Grunerite containing exsolved hornblende

In the grunerite containing exsolved hornblende two sets of exsolution lamellae are visible in the optical microscope (Fig. 2b). These lamellae are visible as large planar features on ($\bar{1}01$) and (100) in the electron microscope (Fig. 5a) and the interface between the lamellae and the grunerite matrix is fully coherent, as is observed in the complementary system. As well as the large (100) lamellae, in some regions there is a low density of medium-sized, coherent particles on ($\bar{1}01$), a low density of medium-sized (100) lamellae and a high density of fine, coherent particles on (100) (Fig. 5a and b). The fine particles are small plates (Fig. 5c) and a PFZ (precipitate-free zone) of the fine plates exists around the larger lamellae. Diffraction patterns from regions containing the (100) plates (Fig. 5d) show reflections from the matrix together with extensive streaking along a^* – the convolution of the Fourier transform of their shape function with reciprocal lattice.

4. Analytical electron microscopy

The analytical electron microscope, EMMA-4, was used to analyse the grunerite lamellae and the hornblende lamellae in sample 1. This instrument has been described elsewhere [10,11] and the application of the instrument to analyse exsolution textures in a bronzite has been discussed in detail by Lorimer and Champness [12]. The instrument is equipped with a probe-forming lens which enables a probe of < 0.1 μm to be formed at the specimen, and, as the sample is thin enough to carry out conventional transmission electron microscopy at 100 kV, $\leqslant 0.3$ μm, a spacial resolution for chemical analysis of

†Pyroxenes are single-chain silicates with the formula $MSiO_3$ where M is Ca, Mg or Fe. Ca-rich pyroxenes, augites, are monoclinic while Ca-poor pyroxenes are either orthorhombic at liquidus temperatures (if the amount of the iron molecule is greater than 30%) or monoclinic (called pigeonites).

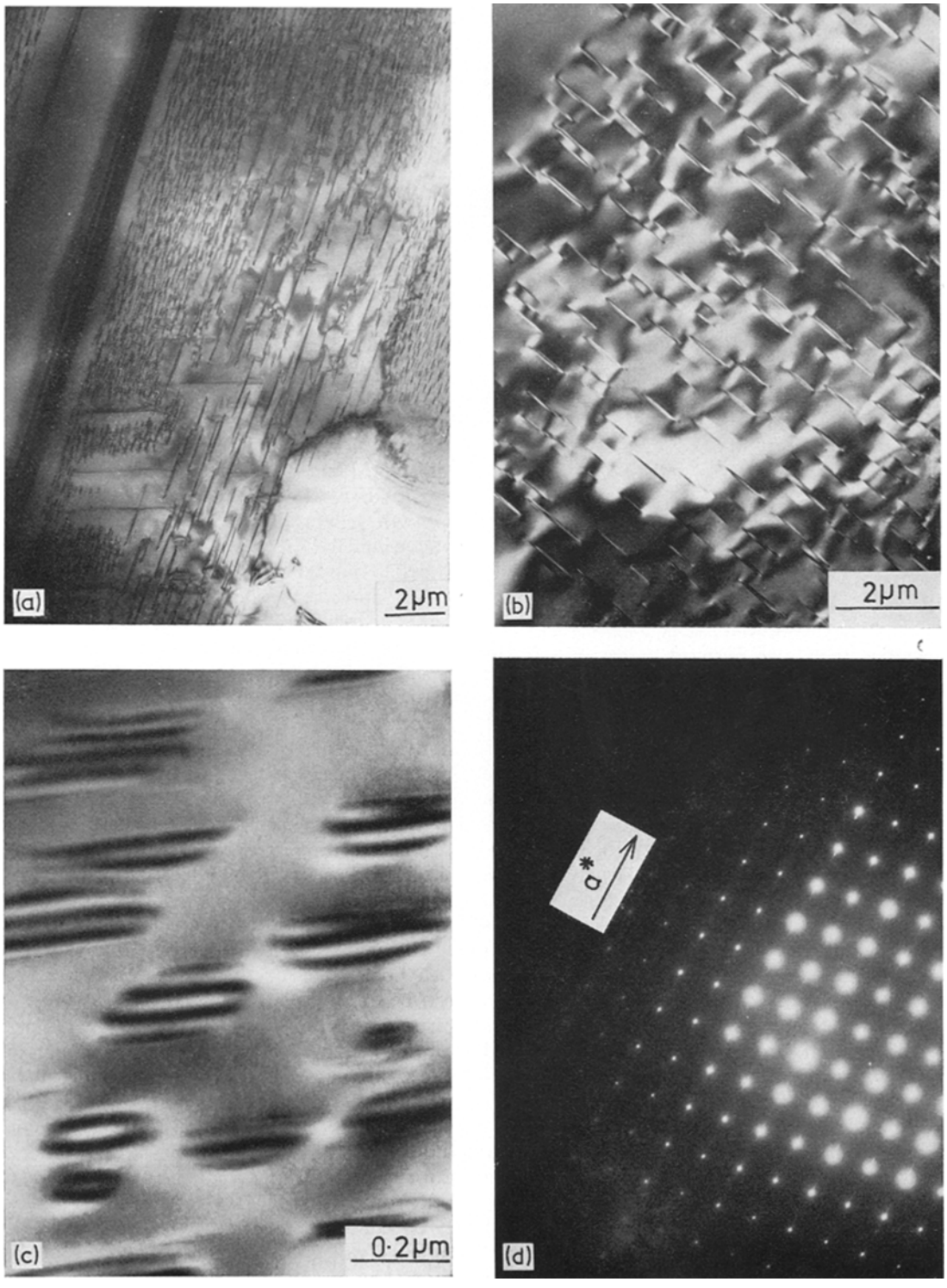

Figure 5 (a) Hornblende lamellae on grunerite with several generations of small lamellae between large (100) lamellae. PFZ of the small lamellae exists adjacent to the larger lamellae. (b) High density of small particles on (100); electron beam approximately parallel to (100). (c) Small particles on (100) viewed with the electron beam making a large angle to (100). The particles are exhibiting displacement fringe contrast. (d) Diffraction pattern from specimen on orientation shown in (c). The streaks in the diffraction pattern are along a^*, perpendicular to the plates.

Figure 6 Hornblende lamellae in grunerite. The contamination spots were produced during analysis with EMMA-4.

approximately 0.1 µm can be obtained. (The position of the probe during an analysis of a grunerite lamellae in hornblende is shown by the contamination marks in Fig. 3a.) The number of X-rays produced is a function of the specimen thickness as well as of the chemical composition and thus absolute X-ray intensities are difficult to convert into chemical weight fractions. However, it has been shown that if the sample is thin enough to carry out transmission electron microscopy at 100 kV, then fluorescence and absorption can be ignored, and the observed X-ray intensity ratios are independent of specimen thickness [11]. During the present investigation the ratio of Ca/Si was determined; as can be seen from Fig. 1, calcium variations would be expected in a hornblende matrix exsolving grunerite or cummingtonite and vice versa, while the silicon weight fraction can be expected to be approximately constant in the matrix and the lamellae. Fig. 6 shows the positions of the probe during the analysis of hornblende lamellae in grunerite.

Fig. 7a and b shows the results of the analyses of hornblende containing grunerite lamellae and grunerite containing hornblende lamellae, respectively. As expected, the grunerite lamellae are calcium-poor in a calcium-rich hornblende matrix and the hornblende lamellae are calcium-rich in a calcium-poor grunerite matrix.

5. Exsolution mechanism

Nucleation of the large exsolution lamellae of hornblende in grunerite or of cummingtonite or grunerite in hornblende can often be seen in the optical microscope to have occurred at interphase boundaries. Growth of the lamellae occurs by the propagation of ledges across the broad, structurally-coherent, lamellae/matrix interfaces. Similar ledges have been observed during the growth of precipitates in a number of metal alloys [13] and their movement has been related quantitatively to the thickening of precipitates. Growth ledges have now been identified on augite lamellae in a bronzite [8] and on pigeonite lamellae in augite [9], and it would appear that ledge movement along broad coherent or semi-coherent interfaces is a general mechanism for the thickening of exsolution lamellae in silicates as well as in metals.

The small coherent (100) precipitate plates observed in the grunerite containing exsolved hornblende have apparently formed by homogeneous nucleation and growth. The PFZ adjacent to the large and medium-sized lamellae in the grunerite indicates that the small precipitates formed after the large and the medium-sized lamellae and that the solute supersaturation adjacent to the lamellae was not sufficiently high for nucleation of the small plates to occur.

The precipitate sequence in either the calcium-rich hornblende or the calcium-poor grunerite can be explained with the aid of the schematic phase diagram shown in Fig. 8. At the temperature of metamorphism, the sample will contain one or two co-existing amphiboles, the volume fraction of each reflecting the initial composition. As the calcium-rich hornblende cools the solubility of Mg and Fe will decrease until the supersaturation is sufficiently high for the heterogeneous nucleation of grunerite lamellae to occur at interphase boundaries. These lamellae will grow, by the migration of ledges across the broad faces of the lamellae until the solute supersaturation is eliminated and/or the temperature falls low enough for diffusion to effectively cease. In the grunerite a similar

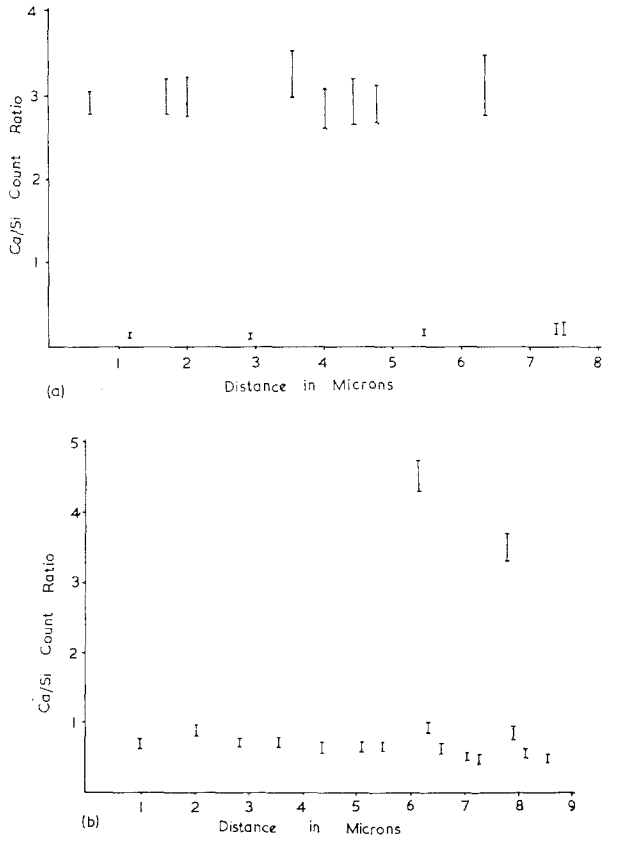

Figure 7 (a) Analysis of a hornblende grain containing grunerite lamellae. (b) Analysis of a grunerite grain containing hornblende lamellae.

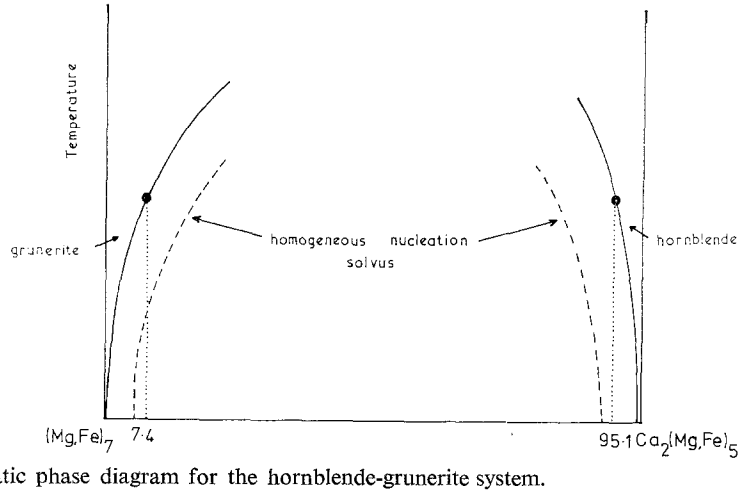

Figure 8 Schematic phase diagram for the hornblende-grunerite system.

precipitation sequence occurs as the temperature falls and the increase in Ca supersaturation results in the heterogeneous nucleation, and the subsequent growth, of calcium-rich hornblende lamellae. At a critical undercooling there is sufficient solute supersaturation for the homo-

geneous nucleation of the fine plates to occur; however, near the heterogeneously-nucleated plates, which have been growing and draining calcium from the matrix as the temperature has decreased, the solute supersaturation is not sufficiently high for homogeneous nucleation to occur and a PFZ is formed. The critical temperature at which homogeneous nucleation occurs can be indicated as a metastable boundary on the phase diagram: above this temperature only heterogeneous nucleation of the lamellae can occur while below it homogeneous nucleation can take place.

A two-stage precipitate distribution – large lamellae and fine coherent precipitates between the lamellae – has been observed in two examples from the pyroxene mineral systems; in an orthopyroxene containing exsolved augite [8] and in a pigeonite containing exsolved augite [14]. In the complementary systems (augite with exsolved orthopyroxene and augite with exsolved pigeonite) only heterogeneously nucleated precipitates have been observed.* In all the cases where homogeneous nucleation has been found, therefore, the formation of a calcium-rich precipitate in a calcium-poor matrix is involved, although the crystallography of the three systems is not analogous (whereas in the case of the amphiboles and clinopyroxenes the two structures are very similar and have the same space group, bronzite is orthorhombic and the augite precipitate is monoclinic). The similarity of the phase distributions in the three cases may reflect the low diffusivity of the large calcium ion. At any specific cooling rate this would result in a high calcium concentration between the heterogeneously-nucleated lamellae and in these regions the calcium supersaturation could become high enough for the homogeneous nucleation of the second phase.

Acknowledgements

The authors would like to thank Professors E. Smith and J. Zussman for providing laboratory facilities. We are extremely grateful to Dr S. O. Agrell and Professor P. Robinson for providing the samples. The high voltage electron microscopy was carried out at the BSC Swinden Laboratories, Rotherham, NERC provided the 100 kV electron microscope and ion thinning machine, and EMMA-4 was purchased with a grant from S.R.C. M.F.G. acknowledges with thanks a maintenance grant from S.R.C.

References

1. W. A. DEER, R. A. HOWIE and J. ZUSSMAN, "Rock-Forming Minerals", Vol. 2 "Chain Silicates" (Longmans, London, 1963).
2. C. KLEIN, *J. Petrol.* **9** (1968) 281.
3. P. ROBINSON, Ph.D. Thesis (1963) Harvard University.
4. D. J. BARBER, *J. Mater. Sci.* **5** (1970) 1.
5. P. E. CHAMPNESS and G. W. LORIMER, *Contr. Mineral. and Petrol.* **33** (1971) 171.
6. M. ROSS, J. J. PAPIKE and K. WIER SHAW, *Min. Soc. Amer. Spec. Pap.* **2** (1969) 275.
7. P. ROBINSON, H. W. JAFFE, M. ROSS and C. KLEIN, *Amer. Mineral.* **56** (1971) 909.
8. P. E. CHAMPNESS and G. W. LORIMER, *J. Mater. Sci.* **8** (1973) 467.
9. P. A. COPLEY, P. E. CHAMPNESS and G. W. LORIMER, *J. Petrol.* in press.
10. C. J. COOKE and P. DUNCUMB, Vth International Conference X-ray Optics and Microanalysis, Tübingen (Springer-Verlag, Berlin, 1968) p. 245.
11. G. W. LORIMER, M. J. NASIR, R. B. NICHOLSON, K. NUTTALL, D. E. WARD and J. R. WEBB, Proceedings of the Vth International Materials Symposium, Berkeley, California (California University Press, Berkeley, 1972) p. 22.
12. G. W. LORIMER and P. E. CHAMPNESS, *Amer. Mineral.* **58** (1973) 243.
13. H. I. AARONSON, C. LAIRD and K. R. KINSMAN, in "Phase Transformations" (A.S.M., Metals Park, 1970) p. 313.
14. P. A. COPLEY, unpublished research.

Received 21 August and accepted 5 September 1973.

Note added in proof: an augite with homogeneously-nucleated pigeonite has recently been found in a rock from the centre of the Whin Sill [14].